Optogenetic methods to study lateralization of synaptic function

Mohamady El-Gaby[1*], Michael M. Kohl[2], Ole Paulsen[1]

[1]*Department of Physiology, Development and Neuroscience, University of Cambridge, Downing Street, Cambridge, UK*
[2]*Department of Physiology, Anatomy and Genetics, University of Oxford, Parks Road, Oxford, UK*

Address for correspondence:
Dr Mohamady El-Gaby
E-mail: mohamady.el-gaby@pharm.ox.ac.uk

University of Oxford
MRC Brain Network Dynamics Unit
Mansfield Road
Oxford, OX1 3TH, UK

or

Dr Michael Kohl
E-mail: michael.kohl@dpag.ox.ac.uk

University of Oxford
Department of Physiology, Anatomy and Genetics
Le Gros Clark Building
South Parks Road
Oxford, OX1 3QX, UK

*Current address: MRC Brain Network Dynamics Unit, University of Oxford, Mansfield Road, Oxford OX1 3TH, UK

ABBREVIATIONS

AAV	adeno-associated virus
AMPAR	α-amino-3-hydroxy-5-methyl-4-isoxazolepropionic acid receptor
Arch	Archaerhodopsin from *Halorubrum sodomense*
ArchT	Archaerhodopsin T from *Halorubrum* strain TP009
CaMKII	Calcium/calmodulin dependent protein kinase II
ChAT	Choline acetyltransferase
ChR2	Channelrhodopsin 2 from *Chlamydomonas reinhardtii*
EPSCs	Excitatory postsynaptic currents
EPSPs	Excitatory postsynaptic potentials
fMRI	Functional magnetic resonance imaging
LTD	Long term depression
LTM	Long term memory
LTP	Long term potentiation
mGluR	Metabotropic glutamate receptor
mRNA	Messenger RNA
MWM	Morris water maze
NpHR	Halorhodopsin from *Natronomonas pharaonis*
NMDAR	*N*-methyl-D-aspartic acid receptor
P2X	Purinoreceptor 2X
PSD	Postsynaptic density
sCRACM	Subcellular ChR2-assisted circuit mapping
STM	Short term memory
TRPV1	Transient receptor potential cation channel subfamily V member 1
VGAT	Vesicular GABA Transporter
VHC	Ventral hippocampal commissure

ABSTRACT

Lateralization of brain function has primarily been studied at the macroscopic level. Studies have detected gross anatomical differences in neuron types, numbers, distribution and connectivity and related these to functional divisions between the two hemispheres. Comparatively little is known about lateralization of synaptic function. A notable exception to this is the recently uncovered lateralization of receptor composition, structure and function of hippocampal Cornu Ammonis (CA)3-CA1 synapses in rodents. Electrophysiological and electron-microscopic studies have revealed that synapses made by the left CA3 onto CA1 neurons on either side of the hippocampus exhibit distinct receptor composition and morphology from those made by the right CA3. Here, we discuss how optogenetic activation and silencing methods have been employed to investigate the consequences of this lateralization for synaptic physiology and circuit organization during learning. The results suggest two general conclusions. First, the spatiotemporal precision of optogenetic tools enables the dissection of lateralization of circuit function in unprecedented detail. Second, seemingly subtle molecular and subcellular lateralizations can translate into prominent differences in circuit function across the hemispheres.

INTRODUCTION

The classical hippocampal trisynaptic circuit ends with one of the most extensively studied synapses in the mammalian central nervous system: the CA3-to-CA1 synapse (**1**; Figure 1). The experimental accessibility of these synapses and their potential importance in memory processing (**2**) have made them a popular target for molecular, electrophysiological and

behavioral studies. In rodents, CA3 pyramidal neurons send excitatory glutamatergic projections both to the ipsilateral CA1 (Schaffer collaterals) and contralateral CA1 (commissural fibers; **1**). Intriguingly, recent data from the mouse hippocampus indicate that inputs originating in the left CA3 form synapses onto CA1 neurons that are functionally distinct from those originating in the right CA3 (henceforth referred to as left-CA3-to-CA1 and right-CA3-to-CA1 synapses respectively; **3-6**). This provides a unique opportunity to investigate the mechanisms and consequences of lateralization at the synaptic level. Before discussing this, however, we begin by briefly introducing the fundamentals of synaptic transmission at CA3-CA1 synapses and describe how synaptic efficacy can change in response to prior activity. We then discuss some of the early evidence for molecular and subcellular lateralization at CA3-CA1 synapses, before motivating the need for more refined techniques, including optogenetics, in order to investigate lateralization of synaptic function.

CA3-CA1 synapses: An introduction

Glutamate is released from *en passant* presynaptic boutons from CA3 pyramidal cells and activates ionotropic glutamate receptors on postsynaptic spines of CA1 pyramidal cells (**1**). The cation permeability of these receptors results in depolarizing currents that can summate to excite CA1 pyramidal neurons. The majority of the resultant depolarization is mediated by the tetrameric α-amino-3-hydroxy-5-methyl-4-isoxazolepropionic acid receptors (AMPARs), while the additional contribution of N-methyl D-aspartate receptors (NMDARs) increases with increasing depolarization of the postsynaptic membrane (**7**; Figure 2). Unlike AMPARs, NMDARs require coincident depolarization-induced relief of a magnesium block and glutamate binding for activation. The high calcium permeability and cytoplasmic C-terminal tail interactions of NMDARs place them at the centre of several intracellular signalling networks that are critical for modulating synaptic function (**7**). In particular, NMDARs are implicated in the induction of activity-dependent changes in synaptic efficacy, known as synaptic plasticity. Strong activation

of NMDARs triggers signalling processes that ultimately mediate long-lasting increases in the efficacy of CA3-CA1 synapses (long-term potentiation; LTP), while weaker activation of these receptors recruits separate mechanisms that reduce synaptic efficacy (long-term depression; LTD; **8**). These processes involve the recruitment of additional AMPARs into the postsynaptic density of CA3-CA1 synapses in the case of LTP, and the removal of these receptors when LTD is induced (**8**). Concomitant changes in spine morphology may occur, with potentiated spines increasing in size and assuming a more mature, mushroom shaped, structure, while depressed spines may shrink (**9**).

A large number of interconnected signaling molecules have been implicated in synaptic plasticity at CA3-CA1 synapses. Of particular note is the calcium/calmodulin dependent protein kinase II (CaMKII), a multimeric enzyme that plays a central role in NMDAR-dependent LTP at CA3-CA1 synapses. Activation of NMDARs and the concomitant calcium influx result in the binding of calcium-calmodulin to CaMKII, which is critical for its activation. CaMKII in turn maintains autonomous activity beyond the initial calcium signal through autophosphorylation, and subsequently phosphorylates and directly binds to a number of targets that mediate the recruitment of AMPARs to the postsynaptic density (PSD) of CA1 spines (**10**). CaMKII is brought to the PSD in part through binding to the C-terminal tail of the GluN2B subunit of NMDARs (**10**). Such an interaction brings CaMKII closer to the transient high calcium microdomains near the channel opening of NMDARs and closer to its target substrates and interacting partners in the PSD. The GluN2B-CaMKII interaction is therefore predicted to be an important modulator of the ability of CA3-CA1 synapses to undergo LTP. In support of this, LTP is impaired in transgenic mice in which the GluN2B-CaMKII interaction is disrupted (**11**; reviewed in **12**). Furthermore, GluN2B levels are higher early in postnatal development, when synapses are in an immature, highly plastic state and diminish with age as synapses mature and become less plastic (**13**). However, a subset of synapses may retain the immature state

into adulthood. Consistent with this, a greater contribution of GluN2B subunit-containing NMDARs to the total NMDAR excitatory postsynaptic currents is seen in small plastic spines compared to large stable spines in the same adult CA1 neurons (**14**, **15**). Thus, a high density of GluN2B subunit-containing NMDARs may serve as a marker of highly plastic synapses.

Lateralization of CA3-CA1 synapses

The first indications of a lateralization of CA3-CA1 synapses came from experiments in which the ventral hippocampal commissure (VHC), a bundle of axons connecting hippocampal subfields across the hemispheres (**1**; Figure 2), was transected to reduce commissural CA3-CA1 connections (**3, 4**). A combination of electrophysiological recordings and immunogold electron microscopy in VHC-transected mice revealed that the left CA3 innervates CA1 spines in which the GluN2B-containing NMDARs contribute more to the total NMDAR current and are of a higher density than in spines innervated by the right CA3 (**3, 4**; Figure 2). Conversely, CA1 spines innervated by the right CA3 exhibit a higher density of GluA1 subunit-containing AMPARs compared to those innervated by the left CA3 (**4**; Figure 2). The morphology of left and right innervated CA1 spines is also different, with the latter being on average larger and more mushroom shaped (**4**; Figure 2). Together, these findings suggest that left-CA3-to-CA1 synapses, with their higher GluN2B density, lower GluA1 density and smaller spine heads, may be in a more immature, plastic state than right-CA3-to-CA1 synapses.

This raises two key questions:

1. To what extent does the molecular and morphological lateralization translate into a difference in plasticity between left-CA3-to-CA1 and right-CA3-to-CA1 synapses?

2. Is there a functional distinction between left and right CA3 in behaving animals as a consequence of the lateralization of CA3-CA1 synapses?

Synaptic plasticity has been primarily studied through electrical stimulation of afferent fibers and intracellular or extracellular recording of excitatory postsynaptic potentials. Such studies have provided critical insights into mechanisms underlying the induction, expression and maintenance of synaptic plasticity. However, the intermingling of distinct subpopulations of afferent fibers, as is the case with afferents from the left and right CA3 in the CA1 of the mouse hippocampus (**1**), means that postsynaptic potentials evoked by electrical stimulation will result from synaptic transmission at various synapses with potentially very different properties. An alternative approach is needed if the properties of these individual components are to be dissected. One solution, already mentioned above, is to transect fiber bundles carrying one set of inputs to the postsynaptic region of interest, thereby allowing the study of one or more sets of inputs in isolation from the transected fibers. Targeting precision can be further improved by restricting stimulation to a particular layer of a subfield. For example, while temporoammonic inputs from the entorhinal cortex arrive onto CA1 pyramidal cell dendrites in the *stratum lacunosum/moleculare*, those from the CA3 are restricted to the *stratum radiatum* and *stratum oriens* (**1**). However, transection of one fiber bundle will rarely leave only one input intact in a CNS circuit. For example, VHC transection, while removing contralateral hippocampal inputs into the CA1, leaves ipsilateral inputs from both the CA3 and CA2 as well as neuromodulatory dopaminergic and noradrenergic inputs into the *stratum radiatum* of the CA1 intact. Another major caveat of this approach is that the prolonged removal of major inputs onto a set of neurons chronically reduces their overall activity. Such a reduction recruits homeostatic mechanisms that keep the overall firing rate of the postsynaptic neurons within a specific dynamic range. For example, prolonged reductions in neuronal firing cause neuron-wide increases in synaptic efficacy, a form of synaptic scaling (**16**). Thus, fiber transection does not merely subtract one set of inputs from an otherwise unchanged repertoire of inputs, but additionally alters the properties of the remaining inputs. This confounds subsequent studies of

synaptic function and especially of synaptic plasticity. These same limitations apply to manipulations in behaving animals aimed at isolating the contribution of CA3-CA1 synapses in one or the other hemisphere. Therefore, there is a need for tools that enable the interrogation of specific inputs within intact circuits if the physiology and behavioral function of these inputs is to be reliably characterized.

In the following sections, we first describe the basic principles of optogenetics and subsequently discuss how both optogenetic activation and silencing have been employed in conjunction with more traditional electrophysiological and behavioral methods to investigate the consequences of the molecular and morphological lateralization at CA3-CA1 synapses. In Section 2, we show that optogenetic activation can be used to isolate left-CA3-to-CA1 or right-CA3-to-CA1 inputs while keeping the rest of the circuitry intact, revealing a dramatic and previously undetected difference in the capacity for LTP between the two sets of synapses. In Section 3, we then describe the use of optogenetic silencing to achieve unprecedented temporal and spatial resolution when interrogating lateralization in the hippocampus of behaving animals. Finally, in Section 4, we outline how hypotheses regarding the development and function of this lateralization can be addressed in future studies by established and newly developed optogenetic approaches.

Section 1 – Optogenetics: An introduction

Optogenetics involves the expression of a class of exogenous, rapidly activated, light-sensitive molecules under the control of cell-type specific promoters to enable manipulation of neuronal activity with high spatiotemporal precision (**17, 18**). Pioneered by Gero Miesenböck's laboratory in 2002, these genetically-targeted, light-sensitive molecules have become an invaluable tool in neuroscience, enabling gain or loss of function within defined neuronal populations on a timescale of milliseconds. The Miesenböck group first used hybrid photoreceptors part-derived from *Drosophila* and combined with G proteins (**19**) to enable robust light-induced depolarization of genetically-targeted vertebrate neurons. They followed this with another approach that combined genetically-targeted expression of a receptor-ion channel with high conductance, such as the vanilloid receptor 1 (transient receptor potential cation channel subfamily V member 1; TRPV1) or purinoreceptor 2X (P2X) channel, with application of a specific, photoactivatable agonist, enabling light-induced activation of these receptors (**20, 21**). Meanwhile, the Isacoff and Kramer laboratories developed an alternative approach that included modifying endogenous ion channels, such as voltage-gated potassium channels (**22**) or ionotropic glutamate receptors (**23**), by attaching a gating molecule or agonist to the ion channel by a light-sensitive tether. A fourth approach, now most widely used in vertebrates, makes use of light-sensitive ion channels derived from algae and bacteria. The Deisseroth lab demonstrated in 2005 that the light-gated cation-selective channel Channelrhodopsin 2 (ChR2) can be expressed in vertebrate neurons and used to depolarize these neurons upon illumination with blue light (**24**). Subsequently, many other microbial opsins were discovered or engineered using site-directed mutagenesis generating a large repertoire of optogenetic molecules with distinct light-sensitivity, conductance, kinetics and expression patterns allowing a high level of flexibility in the types of neuronal manipulations achievable (for review, see **25, 26**).

ChR2 molecules are expressed in the neuronal plasma membrane at the soma as well as dendrites and axon. It is therefore possible to activate particular sub-compartments of neurons through focal light delivery. This has been especially useful for projection targeting, allowing direct activation of axons from genetically and anatomically defined neuronal populations. Furthermore, mutagenesis of ChR2 molecules has generated a battery of variants with distinct properties. For example, the expression of microbial ChR2 in mammalian systems is enhanced by replacing algal codons with mammalian codons, generating the so-called humanised ChR2 (hChR2; **27**). In addition, more targeted mutagenesis of ChR2 has been used to increase conductance (e.g. T159C), increase calcium permeability (e.g. L132C), achieve faster channel closure kinetics and hence improve temporal fidelity (e.g. E123T) or achieve slower channel closure kinetics and hence produce stable 'steps' of depolarization that persist beyond initial light delivery (e.g. C128S; **18**). Several mutations can be combined to achieve hybrid functions. For example, the E123T/T159C hChR2 double mutant exhibits rapid kinetics without the concomitant decrease in photocurrents that is a feature of the E123T single mutant (**28**). This 'ultrafast' variant can therefore produce robust depolarizations that follow relatively high frequency trains of light stimulations with high fidelity (**28**). Nevertheless, there is still an upper limit on the frequency of light pulses that can be reliably followed, which depends partly on the properties of the ChR2 variant and partly on the biophysical properties of the neurons in which they are expressed. The fastest currently available ChR2 variants begin to show unreliable activation at stimulation rates above 40 Hz in pyramidal neurons (**28**). Thus, future modifications are needed to further improve the temporal fidelity of ChR2. In our hands, the hChR2(H134R) (**5**) and the hChR2(E123T/T159C) variants work well to control spiking in excitatory cells or their projections (See Section 2).

In addition to gain-of-function tools, a number of optogenetic loss-of-function tools have been developed. Most notably, the yellow/green-light activated inwards chloride pump halorhodopsin

from *Natronomonas pharaonis* (NpHR; **29**) and the *Halorubrum*-derived yellow/green-light activated proton pumps archaerhodopsin (Arch) and archaerhodopsinT (ArchT; **25, 30**) are capable of effective neuronal silencing through hyperpolarization. These hyperpolarizing tools have been used primarily to rapidly and reversibly silence neurons in order to assess the necessity of activity in defined neuronal populations for distinct behaviors and/or network states (e.g. **6, 31**). Mutagenesis of these proteins has generated a third generation of hyperpolarizing opsins capable of stronger effective photocurrents throughout several neural compartments. Through addition of an endoplasmic reticulum export sequence, and a neurite targeting sequence, third generation NpHR3.0, Arch3.0 and ArchT3.0 exhibit increased targeting to the plasma membrane and enhanced expression in the dendrites and axons compared to their first generation versions (**25**). Thus, they may hold promise for silencing defined axonal projections, such as those made by the CA3 onto the CA1, and hence for assessing their necessity for memory processes. We used successfully eNpHR3.0 to silence spiking of CA3 neurons (**6**; see Section 3). However, in some experiments, especially when studying neural circuits *in vivo*, it may be desirable to optogenetically silence select projections to an area of interest while leaving the activity at the soma and other efferent projections unmodified (See Section 3).

A key power of optogenetics is the capacity to selectively target defined neuronal populations. Such targeting selectivity has been achieved through the generation of transgenic mouse lines that express opsins under the control of cell-type specific promoters. For example, VGAT-ChR2(H134R)-EYFP and ChAT-ChR2(H134R)-EYFP mice exhibit ChR2 expression that is restricted to vesicular GABA transporter (VGAT)-expressing GABAergic neurons or choline acetyltransferase (ChAT)-expressing cholinergic neurons respectively (**18**). Stereotactic injection of viral vectors allows greater flexibility and spatial precision of opsin targeting. One approach is to generate a mouse line that expresses Cre-recombinase, instead of an opsin, under a cell-type specific promoter. Subsequent stereotactic injection of a viral construct expressing the opsin of

choice in a manner that is dependent on Cre-recombinase activity can allow spatial targeting of the opsin to a subset of neurons that express Cre. For example, combining CaMKIIα-Cre mice with stereotactic injection of a Cre-dependent ChR2 viral construct into either the left or right CA3 has allowed analysis of the properties of CA3-CA1 inputs from left or right CA3 pyramidal neurons (**5**). An alternative approach to achieving a high level of spatial and cell-type selectivity is to use viral vectors that express opsins under the control of cell-type specific promoters directly, without the need for transgenic animals. Constructs expressing opsins under the control of excitatory neuron-specific CaMKIIα promoter have been successfully packaged in adeno-associated virus (AAV)-based vectors (**6, 25**). These can be used to target left or right CA3 neurons in wild-type animals (**6**). However, such an approach is limited by the size of constructs that can be packaged into viral vectors, and other neuron-specific promoters, such as the parvalbumin promoter, are too large to include in a construct that fits into an adeno-associated virus. We used both aforementioned viral vector-based approaches to successfully target CA3 neurons in transgenic (**5**) and wild-type (**6**) animals.

Distinct viral vectors and serotypes have different tropisms for neurons, with some infecting cells more readily than others, and thus spreading differently once injected. It is therefore important to choose the appropriate serotype for the manipulation needed. For example, for the *in vivo* silencing of pyramidal neurons in the CA3, we chose the AAV5 serotype (**6**) since it spreads over a larger tissue volume, hence maximizing the percentage of targeted CA3 neurons (**32, 33**). For *ex vivo* electrophysiology experiments, where maximizing virus spread is less critical, we used the more moderately spreading AAV2 serotype (**5**). Furthermore, for some experiments, the spread of AAVs may be less tolerable, for example when the virus is likely to cross laminar borders or when illumination targeting is less feasible. Under these conditions, the pLenti virus, which spreads over a smaller volume, may be preferred (**31**).

To summarize, the recent application of optogenetic tools in mammalian systems has led to a revolution in the interrogation of neural circuits. The high spatiotemporal resolution and flexibility of optogenetic tools make them ideal for investigating the properties and functions of defined populations of neurons and inputs within intact neural circuits. In the following sections, we illustrate the use of optogenetic activation and silencing for investigating hippocampal lateralization.

Section 2 – Optogenetic activation and lateralization of CA3-CA1 synaptic physiology

The lateralization of synaptic composition and morphology at CA3-CA1 synapses raises the possibility that left-CA3-to-CA1 and right-CA3-to-CA1 synapses exhibit distinct physiological properties. In particular, given the importance of GluN2B subunits for LTP and the negative correlation between spine size and LTP capacity, it is possible to propose the following hypothesis:

Hypothesis: The small, GluN2B rich synapses made by the left CA3 onto CA1 neurons exhibit an enhanced capacity for LTP compared to those made by the right CA3.

Two potential caveats need to be addressed before this hypothesis can be tested. Firstly, the lateralization of GluN2B receptor composition is based primarily on data from VHC transected mice (**3, 4**). As discussed before, VHC transection is likely to recruit compensatory changes at the synaptic level that may alter synaptic physiology. Indeed, synaptic GluN2B subunit levels are subject to tight control by prior activity (**13**, **34**), and may thus be altered by the loss of input to CA1 neurons due to VHC transection and/or the resultant synaptic scaling at the intact inputs. A key priority, therefore, is to investigate the possible lateralization of GluN2B subunits at CA3-CA1 synapses and its physiological consequences within intact circuits. The second caveat relates to the mechanistic heterogeneity amongst different forms of LTP. In particular, the degree of block of LTP induction with GluN2B subunit-selective antagonists varies with the LTP induction protocol used (**12**). A careful consideration of this heterogeneity is needed when designing and interpreting LTP experiments with left-CA3-to-CA1 and right-CA3-to-CA1 synapses. We discuss these caveats and how innovative optogenetic activation approaches are beginning to address them.

Optogenetics allows the isolation of defined inputs without the need for fiber transection. The combination of cell-type specificity, offered by expression of opsins under the control of cell-type specific promoters, and anatomical targeting, through the stereotactic injection of viral expression vectors, allows defined neuronal populations and their distinct projections to be interrogated (**18**). Expression of the blue-light activated cation permeable ChR2 allows subsequent light-evoked depolarization of neurons and/or axons. This optogenetic approach is particularly suitable for investigating differences between left-CA3-to-CA1 and right-CA3-to-CA1 synapses for a number of reasons:

1. Left and right CA3 neurons are sufficiently anatomically separated to enable selective stereotactic targeting of viral expression vectors (**1**; Figures 1 and 3).

2. Projections of the CA3 to CA1 neurons are sufficiently separated from CA3 projections to other targets, and from the CA3 soma (**1**), to allow selective activation of CA3-CA1 axons with light sources such as lasers or LEDs (although antidromic spike propagation may reduce this specificity *in vivo*).

3. CA1 pyramidal neurons in mice receive converging intermingled inputs from both left and right CA3 pyramidal neurons (**1**), making the isolation of these two inputs practically impossible in an intact circuit with electrical stimulation, therefore necessitating optogenetic targeting.

4. The large density and laminar organization of CA3 axons in the CA1 enables robust and synchronous excitatory postsynaptic currents (EPSCs) and potentials (EPSPs) to be evoked, which enables reliable detection of changes in synaptic efficacy.

5. Transmission at CA3-CA1 synapses relies on release of small synaptic vesicles which, unlike the large dense core vesicles that mediate release of monoamines and neuropeptides, do not require sustained high frequencies of action potentials for evoked release (**35**). This is important because the frequency with which action potentials can follow trains of light pulses is limited (**18**).

Together, these factors make it possible to use stereotactic viral targeting of opsin expressing constructs (Figure 3) and optogenetically evoke EPSCs and EPSPs at CA3-CA1 synapses that are comparable in size and kinetics to those evoked by conventional electrical stimulation (Figures 4-6).

With optogenetics allowing the isolation of defined synapses, the next challenge is to investigate the receptor composition of these synapses. Whole-cell recording of CA1 pyramidal neurons in voltage-clamp mode allows isolation of AMPAR and NMDAR currents by two types of analyses. Firstly, a magnesium block of NMDARs at resting and hyperpolarized membrane potential results in a negligible contribution of NMDARs to EPSCs at holding voltage negative to -70 mV, allowing isolation of AMPAR currents at these holding voltages (**7**). Secondly, the kinetics of NMDAR currents is slower than that of AMPAR currents (**7**). Thus, at more depolarized membrane potentials, when both AMPARS and NMDARs contribute to EPSCs, the contribution of the latter can be quantified by recording the current after the AMPAR component has decayed but the NMDAR component persists (Figure 4). This voltage clamp-based approach can be combined with increasingly more selective pharmacological tools that enable the isolation not only of AMPAR and NMDAR EPSCs, but also of the contribution of particular subsets of these receptor types through subunit selective blockade or activation. A key example of this is the highly selective blockade of GluN2B subunit-containing NMDARs by ifenprodil and its derivatives (**36**). By combining optogenetics, voltage-clamping and selective pharmacological

blockade, it is possible to investigate the functional glutamate receptor composition at defined synapses within relatively intact networks.

Kohl et al (2011) employed the aforementioned combination of tools to investigate the NMDAR composition of left-CA3-to-CA1 and right-CA3-to-CA1 synapses (**5**; Figure 4). The study made use of a transgenic mouse line expressing Cre-recombinase under the control of the CaMKIIα promoter. This, combined with an AAV2-packaged construct expressing ChR2 in a Cre-dependent manner under the control of the Elongation factor 1α promoter ensured ChR2 expression was restricted to excitatory projection neurons. Stereotactic injection of this construct into the left or right CA3 of adult mice enabled robust expression of ChR2 in CA3 pyramidal neurons and both their ipsilateral and contralateral axonal projections (Figure 3). Whole-cell patch-clamp recordings from CA1 neurons from acute hippocampal slices expressing ChR2 in CA3 projections, and blue-light stimulation in the *stratum radiatum* of the CA1 using a laser enabled recording of AMPAR and NMDAR EPSCs from left-CA3-to-CA1 and right-CA3-to-CA1 synapses in isolation. The study found no left-right difference in the ratio of NMDAR and AMPAR EPSCs (N/A ratio), corroborating findings from VHC transected mice in which both the N/A ratio (when stimulating Schaffer collaterals; **3**) and the relative densities of NMDARs and AMPARs receptors were similar in the left or right hippocampus (**4**, **37**). Crucially, however, application of the ifenprodil derivative Ro 25-6981, to partially block GluN2B-NMDARs, caused a greater reduction of the NMDAR EPSC at left-CA3-to-CA1 compared to right-CA3-to-CA1 synapses (**5**; Figure 4). Thus, the contribution of GluN2B-NMDARs to the total NMDAR current is greater for left-CA3-to-CA1 compared to right-CA3-to-CA1 synapses, confirming earlier findings in VHC transected mice (**3**).

The corroboration of the left-right asymmetry of GluN2B-NMDARs at CA3-CA1 synapses using optogenetic isolation of left-CA3-to-CA1 and right-CA3-to-CA1 inputs opens a window for

investigating the consequences of this lateralization for synaptic plasticity. Given the difference in effectiveness of GluN2B subunit-selective NMDAR antagonists in blocking different forms of LTP, a suitable starting point is to investigate a highly GluN2B-sensitive form of LTP. One such form is timing-dependent LTP (tLTP), which can, for example, be induced by repeated pairings of an EPSP with a burst of three postsynaptic action potentials 5-10 ms later (**38**). This stimulation pattern induces robust, slowly rising LTP (Figure 5). Crucially, tLTP is completely abolished by partial blockade of GluN2B-NMDARs with Ro 25-6981 (**5**). Furthermore, genetic knockout of *Grin2b*, the gene encoding the GluN2B subunit, or knock-in of a version of the *Grin2b* gene lacking the CaMKII binding sites on the GluN2B C-terminal tail replacing the wild-type *Grin2b* gene, abolishes tLTP (**11, 12**). Together, these findings suggest that the induction of tLTP is strongly dependent on GluN2B-NMDARs. Given this strong dependence on GluN2B-NMDARs, Kohl et al (2011) used optical stimulation of ChR2-expressing CA3 afferents in the *stratum radiatum* of the CA1 to assess the induction of tLTP at left-CA3-to-CA1 and right-CA3-to-CA1 synapses, in conjunction with more traditional electrical stimulation. Electrical stimulation, which recruits both Schaffer collateral and commissural CA3-CA1 inputs originating from the left and right CA3, induced identical tLTP in both the left and right CA1 (Figure 4). However, optogenetically isolating CA3-CA1 inputs from one hemisphere revealed that while robust tLTP was induced at left-CA3-to-CA1 synapses, the same induction paradigm failed to induce tLTP at right-CA3-to-CA1 synapses (**5**; Figure 4). This lateralization was apparent when considering CA3 afferents onto the CA1 both ipsilateral and contralateral to the ChR2-expressing CA3. Thus, the potential for tLTP at CA3-CA1 synapses depends strictly on the hemispheric origin of the CA3 afferents, and not the hemispheric location of the postsynaptic CA1 targets.

The left-right asymmetry of tLTP at CA3-CA1 synapses raises an important question: What is the relationship between the lateralization of GluN2B-NMDARs and that of LTP? A simple

possibility is that the lateralization in tLTP is completely explained by the difference in the density of GluN2B subunits and their contribution to the total NMDAR EPSCS between left-CA3-to-CA1 and right-CA3-to-CA1 synapses. This would in turn predict that for less GluN2B sensitive forms of LTP, lateralization would be less apparent or completely absent. One form of LTP that is not blocked by GluN2B-selective NMDAR antagonists is high-frequency stimulation induced LTP (HFS-LTP). Induction of HFS-LTP, typically by presynaptic stimulation at 100 Hz for 1 second, produces a rapidly developing and long lasting potentiation of synaptic transmission (Figure 6). In stark contrast to tLTP, pharmacological blockade of GluN2B-NMDARs has no effect on the long-term component of such potentiation (**39**). Furthermore, HFS-LTP is only partially reduced in *Grin2b* knockin mice lacking the CaMKII binding site (**40**). HFS-LTP is therefore a suitable candidate to test whether the lateralization of LTP at CA3-CA1 synapses extends to paradigms with low sensitivity to selective interference with GluN2B subunits.

The optogenetic induction of HFS-LTP faces a major technical challenge; opsins are limited in their ability to follow high frequency trains of light stimuli for long durations (**18**). Despite the molecular engineering of several 'ultra-fast' ChR2 variants (**28**), the rapid kinetics needed for opsins to follow 100 Hz stimulation for 1 second remain elusive. To bypass this limitation, an alternative approach has been used. Shipton et al (2014) injected an AAV5-packaged construct expressing the hChR2(E123T/T159C) variant under the direct control of the CaMKIIα promoter into the left or right CA3. HFS-LTP was induced in the *stratum radiatum* of the CA1 using conventional electrical stimulation while optogenetic activation of left or right CA3 afferents overlapping with those stimulated electrically allowed the effects of HFS-LTP induction on these distinct inputs to be probed (**6**; Figure 6). Thus, unlike the assessment of tLTP by Kohl et al (2011), Shipton et al (2014) used optogenetics not to induce HFS-LTP, but to monitor left-CA3-to-CA1 or right-CA3-to-CA1 synapses, while HFS-LTP was induced through electrical

stimulation. Surprisingly, the lateralization observed with tLTP was also seen with HFS-LTP; robust HFS-LTP was observed when monitoring left-CA3-to-CA1 synapses but not when monitoring right-CA3-to-CA1 synapses under the same conditions (**6**; Figure 6). As with tLTP, it was the hemispheric origin of the CA3 afferents, rather than that of the CA1 targets, that dictated whether LTP was observed. Thus, lateralization of plasticity at CA3-CA1 synapses extends to LTP paradigms with low sensitivity to GluN2B antagonists.

The lateralization of CA3-CA1 plastic capacity across forms of LTP with distinct induction requirements suggests a fundamental distinction between left-CA3-to-CA1 and right-CA3-to-CA1 synapses (**41**). Indeed, following the initial discovery of a lateralization in GluN2B-NMDARs (**3**), a number of other differences emerged between left-CA3-to-CA1 and right-CA3-to-CA1 synapses. The density of GluA1-containing AMPARs is higher at right-CA3-to-CA1 synapses (**4**). In addition, right CA3 axons synapse onto larger, more mushroom shaped CA1 boutons than those from the left CA3 (**4**). Together, the lateralization in GluA1-AMPAR density and spine morphology suggests that right-CA3-to-CA1 synapses may represent previously potentiated synapses, a feature that would be expected to occlude the expression of subsequent LTP. Furthermore, immunoblotting of the synaptic fraction from the CA1 of VHC transected mice has suggested a larger density of metabotropic glutamate receptor 5 (mGluR5), a key modulator of some forms of LTP (e.g. **42**), at left-CA3-to-CA1 synapses (**37**). Thus, it is likely that distinct molecular features at the level of LTP induction (GluN2B density), expression (GluA1 density and spine size) and modulation (mGluR5 density) cooperate to ensure that left-CA3-to-CA1 synapses are highly plastic while right-CA3-to-CA1 synapses are relatively stable across distinct induction paradigms.

The results described above were derived from recordings in the hippocampal slice preparation. The ease of synaptic recordings and drug delivery in such a preparation has made it highly

popular among researchers studying CA3-CA1 synaptic transmission and plasticity. Furthermore, many of the findings derived from this preparation have been corroborated with *in vivo* recordings in intact animals. However, a number of studies have revealed that the slicing and incubation procedure gives rise to molecular and subcellular changes that alter synaptic physiology. For example, CA1 dendritic spine density increases significantly in slices compared to those in the perfusion-fixed hippocampus (**43**). Similarly, the phosphorylation and activation states of signalling molecules such as CaMKII and protein kinase A and synaptic receptor subunits such as GluA1 are altered in hippocampal slices (**44**). Such changes may alter the function and plasticity of CA3-CA1 synapses. Indeed, the capacity for LTD in adult CA3-CA1 synapses is highly sensitive to the exact slicing and incubation procedure (**44**). These considerations should therefore encourage attempts to investigate lateralization of CA3-CA1 function in intact animals. A major strength of optogenetics is its applicability *in vivo*. Although light scattering is more pronounced in intact tissue, higher light power densities can be easily and safely achieved by high power lasers, allowing reliable activation of neurons and axons *in vivo* (**18**). Corroboration of the findings from hippocampal slices in intact mice would serve to both strengthen existing results and allow more insight into forms of plasticity induced by naturalistic activity patterns and during behaviorally relevant network states.

To summarize, optogenetic activation of axonal projections enables an unprecedented level of spatiotemporal precision and flexibility in addressing synaptic lateralization. The power of this technique was demonstrated in three ways. First, through combining optogenetic activation of CA3-CA1 synapses with NMDAR/AMPAR current recordings and highly selective pharmacological agents, it was possible to directly assess functional receptor composition at defined synaptic inputs in living neurons. This has revealed a higher contribution of GluN2B-NMDARs at left-CA3-to-CA1 compared to right-CA3-to-CA1 synapses. Secondly, optogenetic projection stimulation can be used to specifically potentiate defined inputs, revealing a

preferential induction of tLTP at left-CA3-to-CA1 synapses, and no tLTP induction at right-CA3-to-CA1 synapses. Finally, for situations where optogenetic activation with currently available opsins is incapable of directly inducing potentiation, as is the case with HFS-LTP, optogenetic activation can instead be used to monitor the impact of electrically induced potentiation on distinct inputs. This approach revealed that the left lateralization of LTP at CA3-CA1 synapses extends to HFS-LTP, a form of LTP with low sensitivity to GluN2B-selective NMDAR antagonists. Together, these findings suggest a fundamental lateralization in the capacity for LTP at CA3-CA1 synapses across distinct induction paradigms. However, corroboration of these results *in vivo* and investigations into other forms of plasticity (such as LTD) are necessary in order to fully understand the true extent of functional lateralization at CA3-CA1 synapses.

Section 3 – Optogenetic silencing and lateralization of CA3 function during hippocampus-dependent learning and memory

The hippocampus is a key hub within the mammalian CNS (**45**). Roles in memory processing and spatial navigation have made the hippocampus and its inputs and outputs the subject of intensive physiological and behavioral studies (**46**). Consequently, more details concerning the functional roles of distinct hippocampal neurons are emerging. For example, the granule cells of the dentate gyrus, through their sparse firing and receipt of divergent inputs from the entorhinal cortex, likely perform a pattern separation process, orthogonalizing incoming information in order to minimize interference between neuronal ensembles prior to encoding these memories (**47**). Conversely, the strongly recurrently connected CA3 pyramidal neurons may mediate pattern completion during memory retrieval, recapitulating the full memory ensemble from partial cues (**47**). Together, distinct computations carried out within and between hippocampal subfields are thought to cooperate to mediate memory formation and retrieval.

While the basic hippocampal circuitry is similar between the hemispheres, the recently uncovered difference in synaptic composition, morphology and plasticity between left-CA3-to-CA1 and right-CA3-to-CA1 synapses suggests that these synapses may be part of functionally distinct circuits. In particular, LTP has been strongly implicated in the formation of memories. The synaptic plasticity and memory hypothesis states that *"Activity-dependent synaptic plasticity is induced at appropriate synapses during memory formation, and is both necessary and sufficient for the information storage underlying the type of memory mediated by the brain area in which that plasticity is observed"* (**48**). Several lines of evidence in rodents provide correlative support for this hypothesis. Pharmacological blockade or genetic knockout of NMDARs in the CA1, manipulations that block LTP induction at CA3-CA1 synapses, impairs performance on hippocampus-dependent spatial memory tasks (**49**, **50**, reviewed in **2**). Furthermore, LTP-like

changes in synaptic efficacy and protein phosphorylation in the CA1, and occlusion of further LTP induction at CA3-CA1 synapses are seen with hippocampus-dependent learning (e.g. **51**, reviewed in **2**). These findings are consistent with LTP at CA3-CA1 synapses playing a critical role in memory formation. Given the potential importance of LTP for memory formation, the lateralization in the capacity for LTP at CA3-CA1 synapses across distinct induction paradigms warrants the following hypothesis:

Hypothesis: The plastic left-CA3-to-CA1 synapses are preferentially involved in mediating long-term memory formation. Consequently, left, but not right, CA3 neurons are preferentially required for performance on hippocampus-dependent long-term memory tasks.

Previous studies of functional lateralization in the rodent hippocampus have produced mixed results. For example, Klur et al (2009) used unilateral pharmacological inactivation of either the left or right the hippocampus during training on the Morris water maze (MWM; **52**). While learning of the MWM task was unaffected, performance on a retention probe trial was impaired specifically when left hippocampus was inactivated during the training period (**52**). Conversely, unilateral lesions of the left or right hippocampus in mice caused a similarly small impairment in performance on the MWM, with no evidence of lateralization (**53**). The discrepancy between these and other studies could reflect differences between mice and rats. Alternatively, the lack of lateralization seen in some studies could reflect the nature of the manipulations used. Prolonged manipulations, such as hippocampal lesions, could recruit compensatory synaptic and/or wiring changes that may impact performance on a given task. One dramatic demonstration of this principle was observed when comparing the effects of acute and prolonged silencing of CA1 neurons. While acute CA1 silencing resulted in a profound deficit in recall of remote contextual fear memories, prolonged (30 minutes) silencing of the CA1

produced no deficit (**31**). This lack of an effect of prolonged CA1 silencing was accompanied by an enhanced recruitment of neurons in the anterior cingulate cortex, which may have compensated for the silenced CA1 neurons to mediate accurate memory retrieval (**31**). Thus, acute, trial-limited synaptic silencing is highly desirable to avoid or minimize compensatory changes that alter the processing and/or routing of information through brain circuits.

The speed, reversibility and *in vivo* applicability of optogenetic tools make them of great value when acute manipulations are necessary. Making use of these advantages of optogenetics, Shipton et al (2014) employed an optogenetic neuronal silencing approach as mice learnt a hippocampus-dependent long-term memory (LTM) task. A viral construct expressing the green light-activated chloride pump halorhodopsin (NpHR) under the control of the CaMKIIα promoter was injected into either the left or right CA3 (Figure 3). This produced robust NpHR expression in CA3 pyramidal neurons. For light delivery, an optical cannula was implanted with its tip immediately above the dorsal CA3 in the injected hemisphere (Figure 7). A separate group of mice were injected with a construct expressing the yellow fluorescent protein (YFP) and implanted in the left or right CA3 (as with NpHR injected mice) to serve as controls (Figure 3 and 7). NpHR achieves robust and acute neuronal hyperpolarization suitable for trial limited silencing of neurons (**6, 29, 54**; Figure 7). The authors trained NpHR-expressing, implanted mice on a reference memory Y-maze task. This involved training mice to find a liquid reward in one of three identical arms using extra maze cues for guidance, a task that requires multiple trials across multiple days for mice to learn (Figure 7). Intriguingly, while silencing the right CA3 did not impair task performance, mice in which the left CA3 was silenced were significantly impaired in task acquisition compared to controls (**6**; Figure 7). This did not extend to the hippocampus-independent visual discrimination task, as neither silencing left nor right CA3 impaired task acquisition in this case (**6**). Thus, activity of left but not right CA3 neurons during trial performance is required for acquisition of a hippocampus-dependent LTM task. This is

consistent with the hypothesis that the plastic left-CA3-to-CA1 synapses are preferentially involved in LTM acquisition.

While some evidence suggests that LTP at CA3-CA1 synapses mediates LTM acquisition, less is known about the mechanisms underlying hippocampus-dependent short-term memory (STM). Several lines of evidence point towards a mechanistic dissociation between LTM and STM. For example, while global knockout of the GluA1 or GluN2A subunits of AMPARs and NMDARs respectively impairs hippocampus dependent STM, performance on the MWM, a LTM task, is unaffected (**55, 56**). This may reflect the use of distinct circuits and/or cellular mechanisms by STM and LTM. This would in turn suggest that the relationship between synaptic lateralization and performance on STM tasks may differ from that observed with LTM tasks. Thus, to investigate the possible lateralization of CA3 function during STM tasks, Shipton et al (2014) employed a spontaneous alternation T-maze task (**6, 57**). Mice were placed at the base of a T-shaped enclosure and allowed to explore one of the two other arms for 30 seconds. Subsequently, mice were placed back at the base of the T and again given the choice of entering one of the remaining two arms. Mice are naturally inclined to choose the previously unexplored (alternate) arm in the majority of cases, provided they have formed a memory of visiting the first arm (**57**). In contrast to the clear lateralization of CA3 function during LTM acquisition, Shipton et al (2014) report that NpHR-mediated silencing of left or right CA3 produced a similar impairment in the spontaneous alternation T-maze task (**6,** Figure 7). This lack of lateralization is consistent with a mechanistic difference between LTM and STM and may suggest that networks involving left and right CA3 each contribute unique computations that are necessary for STM performance. Alternatively, it may reflect a higher computational demand for STM, requiring much of the bilateral hippocampal circuitry for task performance. Further experiments will therefore be needed to dissect the mechanisms underlying the necessity for CA3 neurons bilaterally in STM.

Although optogenetic silencing of CA3 neurons with NpHR has been used successfully to address hippocampal function during learning, a number of methodological limitations need to be addressed.

1. Acute optogenetic manipulations provide a powerful way of rapidly interrogating neural circuits with minimal interference from compensatory changes. However, this strength can also be a weakness. The serial interconnectedness, parallel streams of processing, convergence of inputs, and divergence of outputs within neural networks can complicate the interpretation of acute manipulations in one region. This is because for a given node within a network, inputs from other nodes may be playing either an instructive or permissive role. Instructive nodes provide task relevant information to the node of interest for further processing. Other inputs may, however, simply supply a permissive input to the node of interest, for example by providing a 'baseline' level of excitation or by allowing sufficient inhibition to maintain an appropriate excitation/inhibition balance the permits information transfer and/or processing from other nodes (**58**). This becomes important when determining the importance of one neuronal population for relaying *information* necessary for a given task. Silencing a permissive node that does not participate in information processing associated with a task could impair performance of the task simply by disrupting the baseline activity of a downstream node. In the context of lateralization of CA3 function during memory processing, these considerations should encourage a direct assessment of the effects on neuronal information processing in the CA1 as a result of silencing left or right CA3 neurons. We discuss some ways this can be achieved in Section 4.

2. The use of NpHR, a chloride pump, means that in addition to the hyperpolarization produced by influx of chloride ions, the accumulation of intracellular chloride changes the reversal potential of $GABA_A$ receptors such that GABA becomes briefly depolarizing after NpHR

activation (**59**). This results in a pronounced rebound effect in NpHR expressing neurons following light cessation, whereby neuronal spiking transiently increases to levels significantly higher than the pre-light baseline before returning back to baseline levels (**59**; Figure 7). Such an increase in excitation could potentially affect the activity of downstream neurons, which might contribute to the behavioral impairment seen following NpHR-mediated silencing in left CA3 neurons. It will therefore be important to investigate whether CA3 neuronal silencing with other hyperpolarizing tools that do not produce a rebound effect, such as the outward proton pumps Arch and ArchT (**30, 60**), produces the same pattern of behavioral impairment as that seen with NpHR.

3. In addition to Schaffer collateral and commissural projections to the CA1, CA3 pyramidal neurons send projections to other targets including other CA3 pyramidal neurons and interneurons as well as neurons in the lateral septum (**1**). A synapse selective manipulation is therefore necessary in order to make direct links between CA3-CA1 synapses and behaviour. Both halorhodopsin and archaerhodopsin activation at presynaptic terminals can attenuate evoked transmitter release (**61**). However, the exact nature of their effects on synaptic potentials is yet to be characterized.

To conclude, lateralization of plasticity at CA3-CA1 synapses suggests that left-CA3-to-CA1 and right-CA3-to-CA1 synapses may perform distinct functions. This would in turn predict a distinction between left and right CA3 neurons. The acute and highly selective neuronal silencing enabled by the green-light chloride pump NpHR has allowed this prediction to be tested directly. Silencing left but not right CA3 neurons impairs acquisition of a hippocampus-dependent LTM task. Thus, the left CA3, and its plastic inputs onto the CA1, could be part of a lateralized information processing channel participating in computations necessary for LTM during task performance. Interpretation of this result from optogenetic silencing in terms of

information routing should, however, await more detailed interrogation of the exact effects of silencing left CA3 neurons on the activity of neuronal populations in the CA1 and elsewhere within the hippocampal circuitry.

Section 4 – Outstanding questions and methodological ways of addressing them

The findings discussed in this chapter have illustrated how optogenetic activation and silencing are beginning to reveal intriguing insights into the lateralization of synaptic plasticity and memory processes within the hippocampus. Small left-right differences in receptor composition and morphology at CA3-CA1 synapses translate into dramatic differences in plastic capacity, and those distinct types of synapse may in turn participate in distinct computations during learning and memory. The simple and experimentally tractable nature of this lateralization has opened up a number of avenues for research, which we discuss below.

1. Lateralization at CA3-CA1 synapses as a window into determinants of plastic capacity.

The lateralization of plastic capacity suggests a fundamental molecular difference between left-CA3-to-CA1 and right-CA3-to-CA1 synapses. This in turn points towards a tightly regulated developmental programme dedicated to generating this lateralization. Investigating the mechanisms underlying the development of lateralization at CA3-CA1 synapses serves as a unique window into understanding the factors underlying plastic capacity at central synapses since it avoids confounding factors due to cross-region differences in plasticity mechanisms. Spine morphology and receptor composition evolve as an animal develops and are strongly modulated by the history of both presynaptic and postsynaptic neuronal activity (**13, 34**, **62, 63**). NMDARs in immature forebrain synapses of young animals are initially GluN2B rich but are gradually replaced by GluN2A-containing receptors in an activity dependent manner as an animal develops into adulthood (**13**). Furthermore, postsynaptic spine size and synaptic AMPAR density increase in an activity-dependent manner (**63**). This suggests that left-CA3-to-CA1 synapses could be 'trapped' in a less mature state relative to right-CA3-to-CA1 synapses, and indeed compared to the majority of forebrain synapses. Differences in the activity patterns of left and right CA3 neurons during development may have resulted in the preferential maturation of right but not left-CA3-to-CA1 synapses. Alternatively, or perhaps in addition, the sensitivity of

receptor composition and spine morphology at left-CA3-to-CA1 and right-CA3-to-CA1 synapses to neuronal activity could be modulated by lateralized trans-synaptic factors. In order to address these possibilities, a number of approaches can be taken. We summarize some of these below:

A. The activity-dependence of synaptic lateralization can be assessed through extracellular, multi-electrode recordings from left and right CA3 neurons in developing animals to investigate whether differences in activity patterns between left and right CA3 neurons exist. This could be complemented with optogenetic feedback silencing to equalize activity of left and right CA3 neurons and hence assess the necessity of any differences in overall neuronal firing rate for the development of the synaptic lateralization. Furthermore, optogenetic activation of CA3 neurons and/or their projections in isolated left and right hippocampi in a cell culture system could be used to investigate the sufficiency of distinct activity patterns for the development of synaptic lateralization.

B. The involvement of trans-synaptic signalling in mediating the lateralization could be investigated by identifying candidate molecules to target from screens of lateralization in hippocampal gene expression (e.g. **64**), possibly restricted to CA3 pyramidal neurons, combined with genetic knockout studies that abolish the lateralization (e.g. **65**). Hemisphere-specific knockdown of messenger RNA (mRNA) encoding such candidate molecules from left or right CA3-pyramidal neurons could be used to assess their necessity in generating the lateralization. In addition, hemisphere-specific injection of viral constructs expressing candidate molecules to achieve ectopic expression in right or left CA3-pyramidal neurons could be used to assess the sufficiency of these molecules for generating a 'left-CA3-to-CA1 synaptic' phenotype at right-CA3-to-CA1 synapses (or vice versa).

2. Interrogation of synaptic plasticity and integration at the single synapse level

Activation of ChR2-expressing projections using conventional light delivery methods invariably recruits multiple synapses. While this has proved useful for interrogating the averaged plastic capacity of left-CA3-to-CA1 and right-CA3-to-CA1 synapses, an alternative approach is necessary if the properties of single synapses are to be assessed. Such precision is made possible by using ChR2 to directly depolarize individual presynaptic boutons, and hence induce transmitter release, when action potential propagation is pharmacologically blocked (**66**). Direct depolarization of presynaptic boutons can be combined with existing electrophysiological and fluorescent imaging techniques to investigate synaptic plasticity at individual left-CA3-to-CA1 or right-CA3-to-CA1 synapses. This should help elucidate whether plastic capacity is uniform among left-CA3-to-CA1 synapses or whether further sub-distinctions exist among these synapses. Furthermore, an application of this technique, termed subcellular ChR2-assisted circuit mapping (sCRACM), has previously been used to elucidate the dendritic distribution of defined inputs from thalamic nuclei and cortical regions onto target pyramidal neurons in the mouse barrel cortex (**66**). An analogous application of sCRACM to map out the distribution of left-CA3-to-CA1 and right-CA3-to-CA1 synapses in the dendritic tree of CA1 neurons should pave the way for a clearer understanding of how these inputs are integrated at the single neuron level. Overall, functionally interrogating synaptic lateralization at the single synapse level should enable a more refined understanding of functional distinctions between and within populations of left-CA3-to-CA1 and right-CA3-to-CA1 synapses.

3. What network computations are plastic left-CA3-to-CA1 synapses necessary for?

The unique requirement of left but not right CA3 neurons for LTM performance is consistent with a key prediction of the synaptic plasticity and memory hypothesis, namely, that plastic synapses, such as those made by the left CA3 onto the CA1, are necessary for memory storage (**41**, **48**). However, as discussed in Section 3, caution should be taken when interpreting

findings from optogenetic silencing in terms of information routing. A key question therefore is precisely for what aspect of memory storage and/or processing, if any, are plastic left-CA3-to-CA1 synapses necessary?

Hippocampal LTM formation involves a number of mechanistically distinct but coordinated processes. As such, silencing left CA3 neurons could disrupt the encoding, consolidation and/or retrieval of learnt information (**67**). Furthermore, the encoding process itself involves distinct sub-processes, such as spatial map formation and place-reward association (**67, 68**), either or both of which could be disrupted by silencing the left CA3. In order to identify the exact role of left CA3 neurons and their synapses onto the CA1 for performance on long-term memory tasks it will be necessary to interfere with CA3 neuronal activity and/or left-CA3-to-CA1 synaptic activity during distinct phases of task performance. This can involve interference with a distinct phase of each individual trial, for example silencing CA3 neurons only during reward consumption to test their role in reward-place association. In addition, in tasks that are learnt in distinct phases, silencing of left CA3 neurons during blocks of trials comprising a particular phase could enable a more detailed understanding of left CA3 involvement in learning. For example, hippocampus-dependent open-field and maze-based tasks often involve an exploratory phase whereby information regarding the spatial set-up of the context is available but information about reward location is not yet present. This is then followed by trials in which the reward is present at a specific location, and so reward-location associations can be made. The hippocampus has been proposed to play roles in both spatial map formation and associative learning (**69, 70**) and so it will be important to know which, if any, of these processes are dependent on left CA3 neuronal activity. Optogenetic silencing is well suited to such temporally restricted interference owing to its rapid onset and offset. Nevertheless, these tools are not without their caveats. For example, the rebound effect following NpHR activation (see Section 3) could limit its use for temporally restricted, within-trial interference because effects

may extend beyond light cessation. The light-activated proton pumps Arch or ArchT may be more suitable for highly temporally restricted manipulations (**30, 60**). This illustrates the general point that the choice of opsins for behavioral manipulation should be informed by the temporal profile of the physiological effects mediated by each tool, and the characteristics of the desired manipulation.

An approach complementary to understanding the role of left-CA3-to-CA1 synapses is to assess their necessity for hippocampal activity patterns. Pyramidal neurons in the CA3 and CA1 exhibit place cell firing; that is, they are preferentially active at a specific location, or place field, within an environment (**71**). Together, hippocampal place cells can cover an entire environment and have, therefore, been strongly implicated in forming spatial maps of an environment (**69**). Moreover, recent findings have indicated that learning of place-reward associations is accompanied by, and correlates with, changes in the firing rate and/or place field location of place cells (**72, 73**). This learning modulation of place cell firing is especially apparent in the CA1. For example, learning to locate rewards on a cheeseboard maze is accompanied by shifts in place cell firing such that the number of place cells in the CA1 representing goal locations are significantly increased (**73**). These changes could serve as a neural signature for place-reward associations. Coupling optogenetic silencing of left CA3 neurons, or left-CA3-to-CA1 synapses, with place cell recordings could reveal key mechanistic insights into their function. If this causes a specific disruption of learning-induced place cell reorganization, it would indicate that left CA3 neurons, and their outputs onto CA1 neurons, are involved in forming place-reward associations. Conversely, input from left CA3 neurons could be important for CA1 place cell formation and/or stability without necessarily taking part in associative learning (**67**). A further possibility is that the temporal coherence of CA1 place cell populations, a property that correlates with memory performance (**74**), is critically dependent on input from the left CA3. Indeed a recent study provided evidence for a critical role of inputs from the CA3 in the temporal

coding of space within CA1 neuronal ensembles (**75**).Thus, elucidating the effect of interfering with inputs from the left CA3 on CA1 place cell firing patterns during learning is essential for understanding the specific function of these left CA3 neurons and the highly plastic synapses they make in CA1.

4. Hippocampal lateralization in humans

While optogenetic interference is only just beginning to bring some clarity into lateralization of the rodent hippocampus, lateralization of hippocampal function in humans is comparatively better established. Evidence for hippocampal lateralization in humans has come from studies employing virtual reality tasks on healthy volunteers and patients with unilateral hippocampal lesions, in combination with functional magnetic resonance imaging (fMRI; **76**). Early studies revealed that left hippocampal lesions preferentially impair episodic memories while those on the right affect spatial navigation (**76**). While intriguing, such a dissociation poses a key question: What are the underlying differences in the computations performed by left and right hippocampi? A number of subsequent studies have made steps in addressing this question. For example, an fMRI study has shown preferential activation of the left hippocampus when an egocentric strategy was used to solve a spatial navigation task, while allocentric navigation preferentially activated the right hippocampus (**77**). Another fMRI study found that left but not right hippocampal activation reflects associative match-mismatch detection, whereby one of either spatial or temporal arrangements of current sensory stimuli is similar (match) but the other is different (mismatch) to the arrangements of previously encountered inputs (**78**). This suggests that the left hippocampus may be preferentially involved in updating internal representations when incoming sensory input conveys novel information.

Despite the clear examples of hippocampal functional lateralization in humans, the mechanisms contributing to such lateralization are currently unclear. Lateralization of hippocampal

computations in humans suggests a lateralization in underlying network function either within the hippocampal circuitry or at the level of its inputs. However, it is not clear whether the left-right differences in navigation strategies and match-mismatch detection reflect differences in the same fundamental computation, and underlying network processes, or are distinct. This uncertainty is in part due to the lack of clarity regarding the ubiquity of functional lateralization across mammalian species, and hence the lack of adequate, tractable animal models. It is tempting to speculate that the recently uncovered functional lateralization in mouse CA3 function could be related to one or more of the lateralizations discovered in humans. However, it is also possible that lateralization of hippocampal function could have evolved independently in rodents and humans. This uncertainty can be resolved by investigating whether some of the underlying hallmarks of rodent lateralization (e.g. the higher GluN2B density at left-CA3-to-CA1 synapses) are also seen in humans. Given the apparent absence of CA3 projections to the contralateral hemisphere in the posterior hippocampus of humans (**1**), immunohistochemical studies on human *post mortem* tissue might directly reveal subunit composition at left-CA3-to-CA1 and right-CA3-to-CA1 synapses. If rodent and human lateralization is indeed related, further research into the underlying molecular, network and computational underpinnings of the rodent lateralization could have a direct impact on our understanding of human hippocampal lateralization. Conversely, if such lateralizations are fundamentally distinct, this would serve as a useful insight into the different strategies for functional lateralization used by hippocampal networks and their impact on the types of computations the hippocampus and its surrounding networks perform.

Conclusions

This chapter has focused on principles underlying the study of synaptic lateralization, using CA3-CA1 synapses as a case study. Optogenetics has provided a spatiotemporally highly precise means of investigating the properties and functions of defined neuronal and synaptic populations. The rapidly evolving repertoire of optogenetic tools, and their compatibility with various molecular, electrophysiological and behavioral techniques has allowed previously intractable questions to be addressed. Throughout this chapter we have demonstrated distinct ways in which optogenetic activation of CA3-CA1 inputs, or silencing of CA3 neurons, has been employed to investigate the consequences of a molecular and subcellular lateralization at CA3-CA1 synapses. ChR2-mediated optogenetic activation was used both to induce LTP and to monitor the effects of electrically induced LTP on either left-CA3-to-CA1 or right-CA3-to-CA1 synapses. Results from these optogenetic activation studies revealed that left-CA3-to-CA1 synapses have a capacity for LTP that extends across distinct induction paradigms, while right-CA3-to-CA1 synapses are relatively stable. The importance of LTP for long-term memory suggests that plastic left-CA3-to-CA1 synapses are preferentially required for the formation of such memories. Consistent with this hypothesis, NpHR-mediated optogenetic silencing of left but not right CA3 neurons impairs performance on a hippocampus-dependent LTM task. Thus, the seemingly subtle left-right differences in CA3-CA1 synaptic receptor composition translate into dramatic differences in CA3-CA1 plastic capacity and CA3 neuronal function during learning. These findings make important first steps in investigating the mechanisms and consequences of synaptic lateralization. Advances in optogenetic tools and their combination with both new and established molecular, electrophysiological and behavioral techniques promise to further our understanding of the mechanisms and consequences of synaptic lateralization not only at hippocampal CA3-CA1 synapses, but throughout the brain.

ACKNOWLEDGMENTS

References

1) Amaral D, Lavenex P. (2007) Hippocampal neuroanatomy. In: Andersen C, Morris R, Amaral D, Bliss T, O'Keefe J, editors. The hippocampus book. Oxford, England: Oxford University Press. p 4–33

2) Takeuchi T, Duszkiewicz AJ, Morris RG. (2014) The synaptic plasticity and memory hypothesis: encoding, storage and persistence. Philos Trans R Soc Lond B Biol Sci 369(1633):20130288

3) Kawakami R, Shinohara Y, Kato Y, Sugiyama H, Shigemoto R, Ito I. (2003) Asymmetrical allocation of NMDA receptor ε2 subunits in hippocampal circuitry. Science. 300(5621): 990-4.

4) Shinohara Y, Hirase H, Watanabe M, Itakura M, Takahashi M, Shigemoto R. (2008) Left-right asymmetry of the hippocampal synapses with differential subunit allocation of glutamate receptors. Proceedings of the National Academy of Sciences. 105(49):19498–503

5) Kohl MM, Shipton OA, Deacon RM, Rawlins JNP, Deisseroth K and Paulsen O. (2011) Hemisphere-specific optogenetic stimulation reveals left-right asymmetry of hippocampal plasticity. Nature Neuroscience. 14(11):1413-5.

6) Shipton OA, El-Gaby M, Apergis-Schoute J, Deisseroth K, Bannerman DM, Paulsen O, Kohl MM. (2014) Left-right dissociation of hippocampal memory processes in mice. Proc. Natl. Acad. Sci. U S A. 111(42):15238-43

7) Dingledine R, Borges K, Bowie D, Traynelis SF. (1999) The glutamate receptor ion channels. Pharmacol Rev 51(1):7–61.

8) Huganir RL, Nicoll RA. (2013) AMPARs and synaptic plasticity: the last 25 years. Neuron 80(3):704–17.

9) Kasai H, Fukuda M, Watanabe S, Hayashi-Takagi A, Noguchi J. (2010) Structural dynamics of dendritic spines in memory and cognition. Trends Neurosci. 33(3):121-9.

10) Hell JW. (2014) CaMKII: claiming center stage in postsynaptic function and organization. Neuron. 81(2):249-65.

11) Barria A, Malinow R. (2005) NMDA receptor subunit composition controls synaptic plasticity by regulating binding to CaMKII. Neuron. 48(2):289-301.

12) Shipton OA, Paulsen O. (2014) GluN2A and GluN2B subunit-containing NMDA receptors in hippocampal plasticity. Philosophical Transactions of the Royal Society B: Biological Sciences. 369(1633):20130163

13) Yashiro K, Philpot BD. (2008) Regulation of NMDA receptor subunit expression and its implications for LTD, LTP, and metaplasticity. Neuropharmacology. 55(7):1081-94.

14) Matsuzaki M, Honkura N, Ellis-Davies GC, Kasai H. (2004) Structural basis of long-term potentiation in single dendritic spines. Nature. 429(6993):761-6.

15) Sobczyk A, Scheuss V, Svoboda K (2005) NMDA receptor subunit-dependent [Ca2+] signaling in individual hippocampal dendritic spines. Journal of Neuroscience. 25:6037–6046.

16) Turrigiano GG (2008) The self-tuning neuron: synaptic scaling of excitatory synapses. Cell. 135(3):422-35.

17) Miesenbock G, Kevrekidis IG. (2005) Optical imaging and control of genetically designated neurons in functioning circuits. Annu. Rev. Neurosci. 28:533–63.

18) Yizhar O, Fenno LE, Davidson TJ, Mogri M, Deisseroth K. (2011) Optogenetics in neural systems. Neuron. 71(1):9-34.

19) Zemelman BV, Lee GA, Ng M & Miesenböck G (2002). Selective photostimulation of genetically chARGed neurons. Neuron 33, 15–22.

20) Zemelman BV, Nesnas N, Lee GA & Miesenböck G (2003). Photochemical gating of heterologous ion channels: remote control over genetically designated populations of neurons. Proc Natl Acad Sci USA 100, 1352–1357.

21) Lima SQ & Miesenböck G (2005). Remote control of behavior through genetically targeted photostimulation of neurons. Cell 121, 141–152.

22) Banghart M, Borges K, Isacoff E, Trauner D & Kramer RH (2004). Light-activated ion channels for remote control of neuronal firing. Nat. Neurosci. 7, 1381–1386.

23) Szobota S, Gorostiza P, Del Bene F, Wyart C, Fortin DL, Kolstad KD, Tulyathan O, Volgraf M, Numano R, Aaron HL, Scott EK, Kramer RH, Flannery J, Baier H, Trauner D & Isacoff EY (2007). Remote control of neuronal activity with a light-gated glutamate receptor. Neuron 54, 535–545.

24) Boyden ES, Zhang F, Bamberg E, Nagel G & Deisseroth K (2005). Millisecond-timescale, genetically targeted optical control of neural activity. Nat. Neurosci. 8, 1263–1268.

25) Mattis J, Tye KM, Ferenczi EA, Ramakrishnan C, O'Shea DJ, Prakash R, Gunaydin LA, Hyun M, Fenno LE, Gradinaru V, Yizhar O, Deisseroth K (2012) Principles for applying optogenetic tools derived from direct comparative analysis of microbial opsins. Nat. Methods 9:159–172

26) Deisseroth K (2015). Optogenetics: 10 years of microbial opsins in neuroscience. Nat Neurosci 18, 1213–1225.

27) Zhang F, Wang LP, Boyden ES, Deisseroth K. (2006) Channelrhodopsin-2 and optical control of excitable cells. Nature Methods. 3(10):785-92.

28) Gunaydin LA, Yizhar O, Berndt A, Sohal VS, Deisseroth K, Hegemann P. (2010) Ultrafast optogenetic control. Nat. Neurosci. 13(3):387-92.

29) Zhang F, Wang LP, Brauner M, Liewald JF, Kay K, Watzke N, Wood PG, Bamberg E, Nagel G, Gottschalk A, Deisseroth K. (2007) Multimodal fast optical interrogation of neural circuitry. Nature. 446(7136):633-9.

30) Chow BY, Han X, Dobry AS, Qian X, Chuong AS, Li M, Henninger MA, Belfort GM, Lin Y, Monahan PE, Boyden ES. (2010) High-performance genetically targetable optical neural silencing by light-driven proton pumps. Nature. 463(7277):98-102.

31) Goshen I, Brodsky M, Prakash R, Wallace J, Gradinaru V, Ramakrishnan C, Deisseroth K. (2011) Dynamics of retrieval strategies for remote memories. Cell. 147(3):678–89.

32) Aschauer DF, Kreuz S & Rumpel S (2013). Analysis of Transduction Efficiency, Tropism and Axonal Transport of AAV Serotypes 1, 2, 5, 6, 8 and 9 in the Mouse Brain ed. Qiu J. PLoS ONE 8, e76310.

33) Watakabe A, Ohtsuka M, Kinoshita M, Takaji M, Isa K, Mizukami H, Ozawa K, Isa T & Yamamori T (2015). Comparative analyses of adeno-associated viral vector serotypes 1, 2, 5, 8 and 9 in marmoset, mouse and macaque cerebral cortex. Neurosci Res 93, 144–157.

34) Lee MC, Yasuda R, Ehlers MD. (2010) Metaplasticity at single glutamatergic synapses. Neuron. 66(6):859-70.

35) Zucker RS, Kullmann DM, Kaeser PS. (2014) Release of Neurotransmitters. In: Byrne J, Heidelberger R and Waxham MN From Molecules to Networks (Third Edition): An Introduction to Cellular and Molecular Neuroscience. Cambridge, USA: Academic Press p 443-88.

36) Paoletti P, Neyton J. (2007) NMDA receptor subunits: function and pharmacology. Curr Opin Pharmacol. 7(1):39-47.

37) Shinohara Y, Hirase H. (2009) Size and receptor density of glutamatergic synapses: a viewpoint from left-right asymmetry of CA3-CA1 connections. Front Neuroanat. 3:10.

38) Pike FG, Meredith RM, Olding AW, Paulsen O (1999), "Rapid report: postsynaptic bursting is essential for 'Hebbian' induction of associative long-term potentiation at excitatory synapses in rat hippocampus." J Physiol 518 (Pt 2):571-6.

39) Volianskis A, Bannister N, Collett VJ, Irvine MW, Monaghan DT, Fitzjohn S, Jensen MS, Jane DE, Collingridge GL. (2012) Different NMDA receptor subtypes mediate induction of long-term potentiation and two forms of short-term potentiation at CA1 synapses in rat hippocampus in vitro. J. Physiol. 591, 955–972.

40) Halt AR, Dallapiazza RF, Zhou Y, Stein IS, Qian H, Juntti S, Wojcik S, Brose N, Silva AJ, Hell JW (2012) CaMKII binding to GluN2B is critical during memory consolidation. EMBO 31:1203–1216.

41) El-Gaby M, Shipton OA, Paulsen O. (2015) Synaptic plasticity and memory: new insights from hippocampal left-right asymmetries. Neuroscientist. 21(5):490-502

42) Kwag J, Paulsen O. (2012) Gating of NMDA receptor-mediated hippocampal spike timing-dependent potentiation by mGluR5. Neuropharmacology. 63(4):701-9.

43) Kirov SA, Sorra KE, Harris KM. (1999) Slices have more synapses than perfusion-fixed hippocampus from both young and mature rats. J Neurosci. 19(8):2876-86.

44) Ho OH, Delgado JY, O'Dell TJ. (2004) Phosphorylation of proteins involved in activity-dependent forms of synaptic plasticity is altered in hippocampal slices maintained in vitro. J Neurochem. 91(6):1344-57.

45) Battaglia FP, Benchenane K, Sirota A, Pennartz CM, Wiener SI. (2011) The hippocampus: hub of brain network communication for memory. Trends Cogn Sci. 15(7):310-8.

46) Andersen C, Morris R, Amaral D, Bliss T, O'Keefe J, editors. 2007. The hippocampus book. Oxford, England: Oxford University Press.

47) Rolls ET. (2015) Pattern separation, completion, and categorisation in the hippocampus and neocortex. Neurobiol Learn Mem. pii: S1074-7427(15)00129-X.

48) Martin SJ, Grimwood PD, Morris RG. (2000) Synaptic plasticity and memory: an evaluation of the hypothesis. Annu Rev Neurosci 23:649–71.

49) Morris RG, Anderson E, Lynch GS, Baudry M. (1986) Selective impairment of learning and blockade of long-term potentiation by an N-methyl-D-aspartate receptor antagonist, AP5. Nature. 319(6056):774-6.

50) Tsien JZ, Huerta PT, Tonegawa S. (1996) The essential role of hippocampal CA1 NMDA receptor-dependent synaptic plasticity in spatial memory. Cell. 87(7):1327-38.

51) Whitlock JR, Heynen AJ, Shuler MG, Bear MF. (2006) Learning induces long-term potentiation in the hippocampus. Science. 313(5790):1093-7.

52) Klur S, Muller C, Pereira de Vasconcelos A, Ballard T, Lopez J, Galani R, Certa U, Cassel JC (2009) Hippocampal-dependent spatial memory functions might be lateralized in rats: An approach combining gene expression profiling and reversible inactivation. Hippocampus 19:800–816.

53) Gerlai RT, McNamara A, Williams S, Phillips HS(2002) Hippocampal dysfunction and behavioral deficit in the water maze in mice: an unresolved issue? Brain Research Bulletin 57:3–9.

54) Gradinaru V, Zhang F, Ramakrishnan C, Mattis J, Prakash R, Diester I, Goshen I, Thompson KR, Deisseroth K (2010) Molecular and cellular approaches for diversifying and extending optogenetics. Cell141:154–165.

55) Reisel D, Bannerman DM, Schmitt WB, Deacon RM, Flint J, Borchardt T, Seeburg PH, Rawlins JN (2002) Spatial memory dissociations in mice lacking GluR1. Nat. Neurosci. 5:868–873.

56) Bannerman DM, Niewoehner B, Lyon L, Romberg C, Schmitt WB, Taylor A, Sanderson DJ, Cottam J, Sprengel R, Seeburg PH, Köhr G, Rawlins JN.. (2008) NMDA receptor subunit NR2A is required for rapidly acquired spatial working memory but not incremental spatial reference memory. J. Neurosci. 28:3623–3630.

57) Deacon RM, Rawlins JN. (2006) T-maze alternation in the rodent. Nat Protoc. 1(1):7-12.

58) Otchy TM, Wolff SB, Rhee JY, Pehlevan C, Kawai R, Kempf A, Gobes SM, Ölveczky BP. (2015) Acute off-target effects of neural circuit manipulations. Nature. 528(7582):358-63.

59) Raimondo JV, Kay L, Ellender TJ, Akerman CJ. (2012) Optogenetic silencing strategies differ in their effects on inhibitory synaptic transmission. Nat Neurosci. 15(8):1102-4.

60) Han X, Chow BY, Zhou H, Klapoetke NC, Chuong A, Rajimehr R, Yang A, Baratta MV, Winkle J, Desimone R, Boyden ES. (2011) A high-light sensitivity optical neural silencer:

development and application to optogenetic control of non-human primate cortex. Front. Syst. Neurosci. 5:18.

61) Mahn M, Prigge M, Ron S, Levy R, Yizhar O. (2016) Biophysical constraints of optogenetic inhibition at presynaptic terminals. Nat Neurosci. 19(4):554-6.

62) Abraham WC. (2008) Metaplasticity: tuning synapses and networks for plasticity. Nat Rev Neurosci. 9(5):387.

63) Hanse E, Seth H, Riebe I. (2013) AMPA-silent synapses in brain development and pathology. Nat Rev Neurosci. 14(12):839–50.

64) Moskal JR, Kroes RA, Otto NJ, Rahimi O, Claiborne BJ. (2006) Distinct patterns of gene expression in the left and right hippocampal formation of developing rats. Hippocampus.16(8):629-34.

65) Kawahara A, Kurauchi S, Fukata Y, Martínez-Hernández J, Yagihashi T, Itadani Y, Sho R, Kajiyama T, Shinzato N, Narusuye K, Fukata M, Luján R, Shigemoto R, Ito I. (2013) Neuronal major histocompatibility complex class I molecules are implicated in the generation of asymmetries in hippocampal circuitry. J Physiol 591(19):4777–91

66) Petreanu L, Mao T, Sternson SM, Svoboda K. (2009) The subcellular organization of neocortical excitatory connections. Nature. 457(7233):1142-5.

67) Kandel ER, Dudai Y, Mayford MR. (2014) The molecular and systems biology of memory. Cell. 157(1):163-86.

68) de Lavilléon G, Lacroix MM, Rondi-Reig L, Benchenane K. (2015) Explicit memory creation during sleep demonstrates a causal role of place cells in navigation. Nat. Neurosci..18(4):493-5.

69) O'Keefe J, Nadel L. 1978. The hippocampus as a cognitive map. Oxford, England: Oxford University Press.

70) Eichenbaum H, Cohen NJ. (2014) Can we reconcile the declarative memory and spatial navigation views on hippocampal function? Neuron. 83(4):764-70.

71) O'Keefe J, Dostrovsky J. 1971. The hippocampus as a spatial map. Preliminary evidence from unit activity in the freely moving rat. Brain Res 34(1):171–5.

72) Hollup SA, Molden S, Donnett JG, Moser MB, Moser EI. (2001) Accumulation of hippocampal place fields at the goal location in an annular watermaze task. J Neurosci 21(5): 1635–44.

73) Dupret D, O'Neill J, Pleydell-Bouverie B, Csicsvari J. (2010) The reorganization and reactivation of hippocampal maps predict spatial memory performance. Nature Neuroscience. 13(8):995-1002.

74) Buzsáki G, Moser EI. (2013) Memory, navigation and theta rhythm in the hippocampal-entorhinal system. Nat. Neurosci. 16(2):130-8.

75) Middleton SJ, McHugh TJ. (2016) Silencing CA3 disrupts temporal coding in the CA1 ensemble. Nat Neurosci. doi: 10.1038/nn.4311. [Epub ahead of print]

76) Burgess N, Maguire EA, O'Keefe J. (2002) The human hippocampus and spatial and episodic memory. Neuron 35(4):625–41.

77) Iglói K, Doeller CF, Berthoz A, Rondi-Reig L, Burgess N. (2010) Lateralized human hippocampal activity predicts navigation based on sequence or place memory. Proc Natl Acad Sci U S A 107(32):14466–71.

78) Kumaran D, Maguire EA. (2007) Match mismatch processes underlie human hippocampal responses to associative novelty. J Neurosci 27(32):8517–24.

FIGURE LEGENDS

Figure 1: Schematic of the rodent hippocampal circuit. Granule cells in the dentate gyrus (DG) project onto pyramidal neurons in the CA3. These in turn send bilateral excitatory glutamatergic projections to pyramidal neurons in the CA1.

Figure 2: Composition and lateralization of CA3-CA1 synapses. Schematic representation of glutamatergic synapses at CA1 pyramidal neurons innervated by left or right CA3 axons. Left CA3 inputs innervate dendritic spines of lower volumes than their right counterparts. Furthermore, the postsynaptic densities (PSDs) of spines receiving right CA3 inputs are larger in area than those receiving left CA3 inputs. The PSDs of spines innervated by left CA3 inputs have a higher density of GluN2B-containing NMDARs and a lower density of GluA1-containing AMPARs than those receiving right CA3 inputs. The C-terminal tails of GluN2B subunits contain high affinity binding sites for CaMKII. These can be occupied at the basal state or can serve as docking sites for the recruitment of CaMKII in response to LTP-inducing stimuli, thereby bringing CaMKII close to its substrates and enabling LTP. The densities of GluA2 and GluA3 subunits do not differ between the two types of inputs and hence their total numbers scale with the area of the PSD.

Figure 3: Unilateral stereotactic targeting of viral constructs encoding opsins and matched controls to the CA3. A) (Left) Schematics of gene constructs encoding enhanced yellow fluorescent protein (eYFP) or eYFP-fused to the third generation halorhodopsin from *Natronomonas pharaonis* (NphR3.0) under the control of the CaMKIIα promoter to restrict expression to excitatory neurons. The woodchuck hepatitis posttranscriptional regulatory element (WPRE) is added to enhance gene expression. (Middle) Gene construct encoding channelrhodopsin-2 (ChR2)-eYFP under the control of the EF1α promotor. When expressed, the Cre-recombinase enzyme catalyzes recombination at LoxP and Lox2722 sites resulting in the inversion of the construct which becomes in frame with the EF1α promoter and hence competent for expression. (Right) Adeno-associated viruses (AAV) containing one of these constructs are then injected into the left or right CA3 of wild-type C57BL/6 mice (Cre-independent constructs) or CaMKIIα-Cre mice (Cre-dependent constructs) using stereotactic

apparatus. B) (Left) An immunofluorescence image of a coronal slice from a mouse injected with an AAV containing a ChR2-eYFP construct. The viral injection site is marked by red beads. Expression of ChR2-eYFP, detected using an antibody against eYFP, is prominent in the CA3 and its projections to the ipsilateral and contralateral CA3 and CA1. (Right) Only pyramidal neurons (CaMKIIα expressing; arrowheads) in the ipsilateral CA3 region expressed ChR2-eYFP. s.l., stratum lucidum; s.r., stratum radiatum; s.o., stratum oriens. Panel B adapted from (**5**).

Figure 4: Optogenetic activation reveals lateralized GluN2B-NMDAR contribution at CA3-CA1 synapses. A) Optogenetic activation set up. A CA1 pyramidal neuron is patched in whole-cell patch mode and its responses monitored in voltage-clamp. A high-power laser is used to deliver 473 nm light to a focal point within the CA1 stratum radiatum in coronal hippocampal slices expressing ChR2 in CA3 projections (either Schaffer collateral or commissural) from either the left or right CA3. B) The voltage-clamp recording protocol consists of alternating 3-second steps to -90 mV and 60 mV, returning to -90 mV in between. Each recorded sweep is 4 seconds, and there is 14 seconds between each stimulation (red line), which is delivered 2 seconds into each sweep to evoke an EPSC. In order to measure series resistance, a 5 mV test pulse of 100ms duration is delivered at the start of each recording sweep. C) Example EPSC traces. The AMPAR-mediated current is estimated using the peak amplitude at -90 mV (black dashed line) and the NMDAR-mediated current is estimated at a time window of 55-57 ms after stimulation (grey dashed line), at a time when the AMPAR-mediated component has decayed to less than 5% of its peak value. D) (Left) There was no difference in the overall NMDA/AMPA ratios between left and right for either electrical or optical stimulation (dark gray box indicates the time window for estimation of the NMDAR current). (Right) Selective block of GluN2B subunit–containing NMDARs with 0.5 μM Ro 25-6981 affected the NMDAR current evoked by left CA3 input more than that evoked by right CA3 input. Open bars indicate NMDAR current estimate in control, filled bars indicate remaining NMDAR current in the presence of 0.5 μM Ro 25-6981. Traces show representative optically evoked postsynaptic currents at +60 mV in the presence of 0.5 μM Ro 25-6981 for left and right CA3-injected animals. Panel A adapted from (**6**), panel D adapted from (**5**).
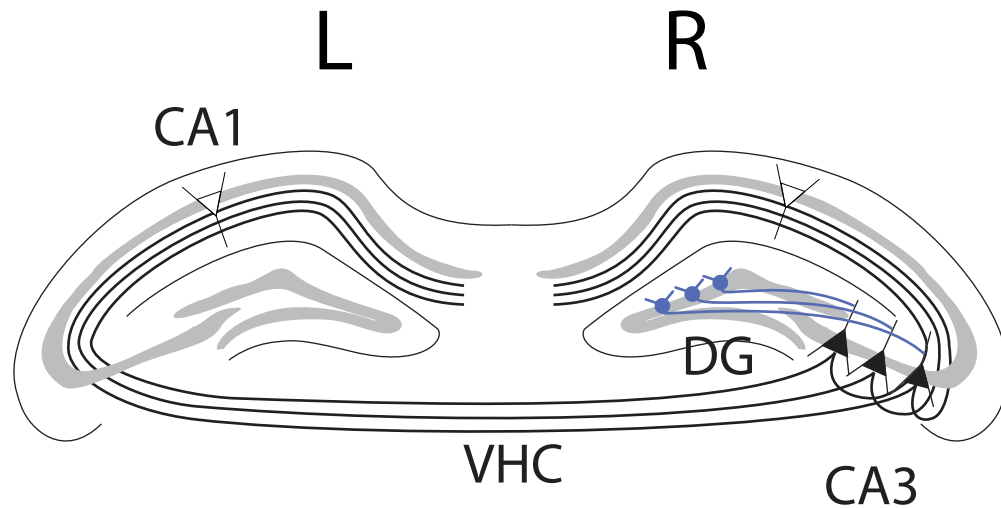
Figure 5: Optogenetic activation reveals lateralization of t-LTP at CA3-CA1 synapses. A) Optogenetic activation set up. A CA1 pyramidal neuron is patched in whole-cell mode and its responses monitored in current-clamp. A high power laser is used to deliver 473 nm light to a focal point within the CA1 stratum radiatum in coronal hippocampal slices expressing ChR2 in CA3 projections from either the left or right CA3. Electrical stimulation is also delivered to the stratum radiatum of the CA1 at a separate set of fibers. B) Protocol for inducing t-LTP. Optical stimulation at CA3 axons in the stratum radiatum of the CA1 induces excitatory postsynaptic potentials in CA1 pyramidal neurons (top). To induce t-LTP, single EPSPs are paired with a burst of three postsynaptic action potentials evoked by direct current injection into the patched pyramidal neuron (bottom). C) Indiscriminate electrical stimulation (triangles) in the stratum radiatum produced robust t-LTP in CA1 pyramidal neurons. Selective optical stimulation (circles) of CA3 Schaffer collaterals (ipsilateral projections) and commissural fibers (contralateral projections; not shown) originating in the left hemisphere also both induced t-LTP. In contrast, optical stimulation of CA3 projections originating in the right hemisphere led to significantly less t-LTP than electrical stimulation. Insets show representative EPSPs at the indicated time points (1, 2). Panel A adapted from (**6**), panel C adapted from (**5**).

Figure 6: Optogenetic activation reveals lateralization of HFS-LTP at CA3-CA1 synapses. A) Projections from the CA3 in the injected hemisphere that express ChR2 are activated by optical stimulation in the stratum radiatum via blue (470 nm) light delivered from a high-power LED coupled to a 200 μm fiber. These projections are either hippocampal Schaffer collateral or commissural projections depending on whether the slice used is ipsilateral or contralateral to the injected hemisphere. Electrical stimulation recruits expressing and non-expressing projections indiscriminately. The optical fiber and stimulation electrode are placed as closely as possible so that light and electrical stimulation recruit some of the same projections. Overlapping electrical and optical stimulation in the stratum radiatum enables the effect of high-frequency, electrical stimulation (HFS) to be measured on selective optical stimulation. The fEPSP response is monitored by a glass recording pipette containing artificial cerebrospinal fluid (aCSF) in the stratum radiatum. B) The induction protocol consists of a tetanus of 100 electrical stimulations at 100 Hz. The gray inset window shows an example field response to the first 10 stimuli of the high-frequency induction protocol. C) Top: HFS (arrows) produced robust LTP in the electrical pathway (black triangles), but the optical pathway (circles) only showed LTP when projections
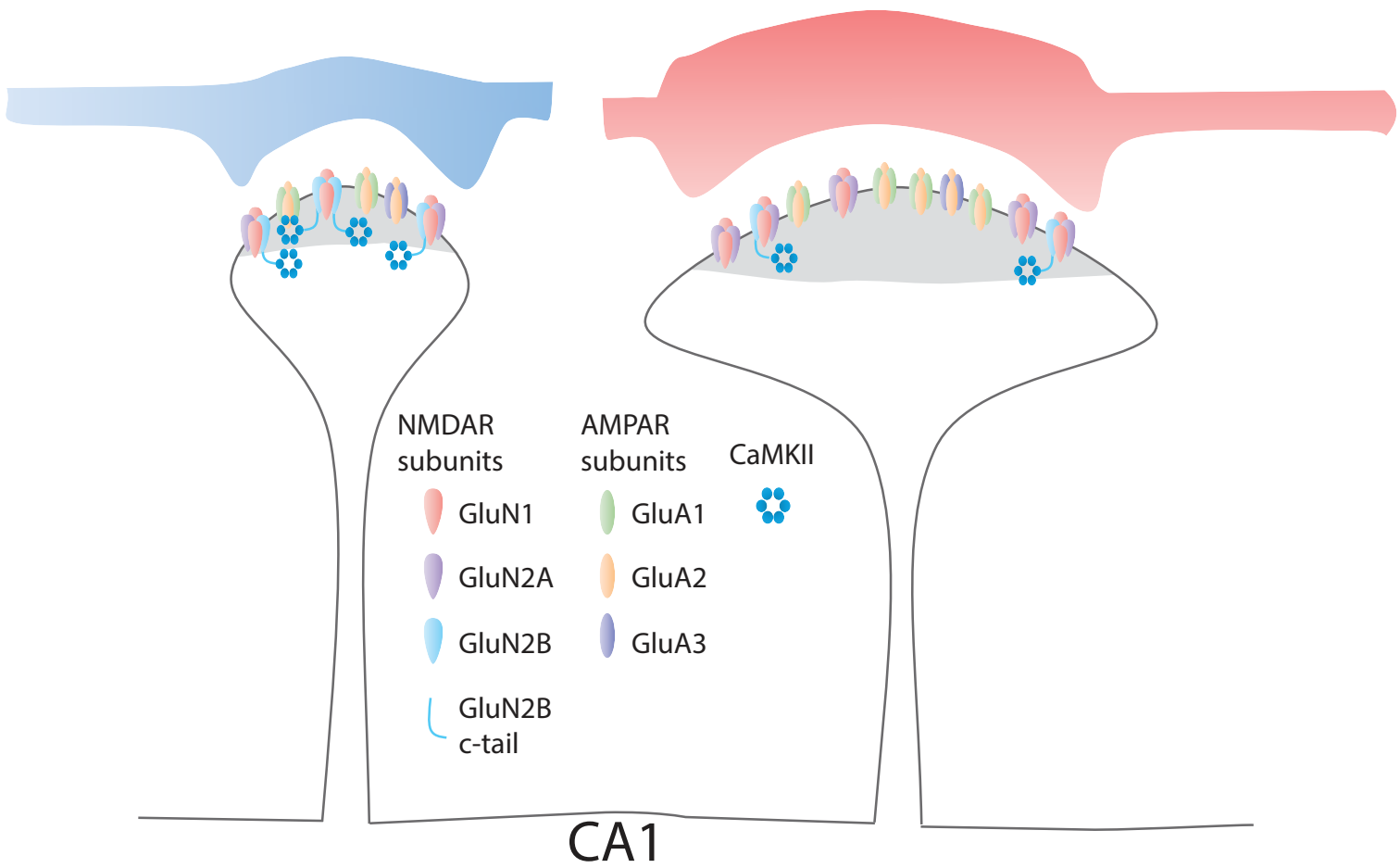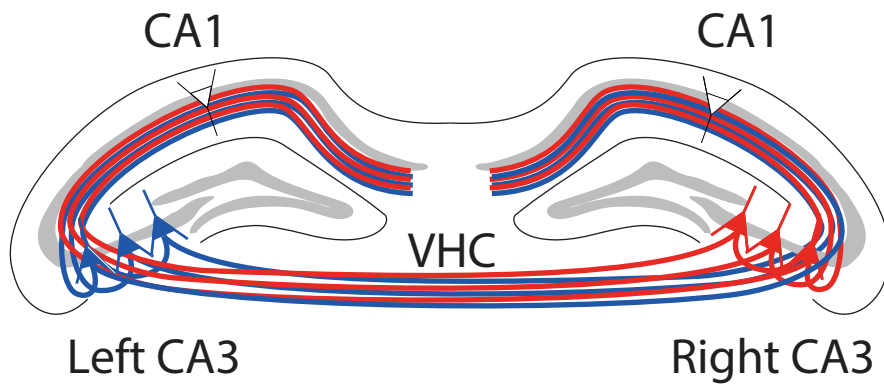
originated in the left CA3. Insets show representative fEPSPs at the indicated time points (1, 2).Bottom: Significantly more LTP was observed in left-injected mice than in right-injected mice in the optical pathway. Broken lines represent baseline. Error bars represent s.e.m. ** P<0.01. Panel A and C adapted from (**6**).

Figure 7: Optogenetic silencing reveals lateralization of CA3 function during long-term, but not short-term, memory performance. A) Top: Mice received unilateral CA3 injection of an AAV construct containing either eNpHR3.0-eYFP or eYFP only. An optical fiber contained in a metal cannula (red arrow) was inserted into the brain above the AAV-injected CA3 and secured to the skull using dental cement (blue arrow). Bottom: Green (532nm) laser light was coupled to the inserted optical fiber and delivered to the CA3. B) Illumination of CA3 neurons in anesthetized mice with green laser light for 30 seconds resulted in a reversible reduction in spontaneous spiking. The graph shows the normalized mean frequency of spiking. Grey window depicts one period of silencing. Green bars depict time with light on. Note the rebound activity observed at light off set (**59**). C) Elevated Y-maze task. Left: Mice were trained to find the rewarded arm (+), which remained in a fixed location relative to extra-maze cues, following release from one of the two start arms (S) allocated through a pseudorandom sequence. Mice entering the non-rewarded arm (–) were removed from the maze. Light was delivered throughout the trial. Middle: Mice received blocks of 10 trials a day for eleven days and the number of correct arm entries was recorded each day. The performance of all four groups of mice improved over the course of testing, but to a different extent. On the final day of testing, the reward was given after the arm choice was made (post-choice baiting, P.C.B.). Broken lines represent chance performance of 50%. Light delivery in mice injected with NpHR in the left CA3 (left-NpHR, blue) impairs their learning of reward location, but does not affect learning in right-NpHR mice (red) and control groups (left-eYFP: black, right-eYFP: gray). Right: The average performance on the penultimate day. Broken lines represent chance performance of 50%. D) Spontaneous alternation T-maze task. Left: Mice were placed in the start arm (S) and allowed to make a free choice of arm. Once they entered an arm, a barrier was put in place so that they explored the chosen arm for 30 seconds. Mice were then removed and placed immediately back in the start arm and the next arm choice was recorded. If mice chose the novel arm, this was counted as a spontaneous alternation. Right: The average rate of alternation in the light-on condition. Broken line represents chance performance of 50%. Light delivery reduces performance of both right-NpHR and left-NpHR mice compared to their respective eYFP
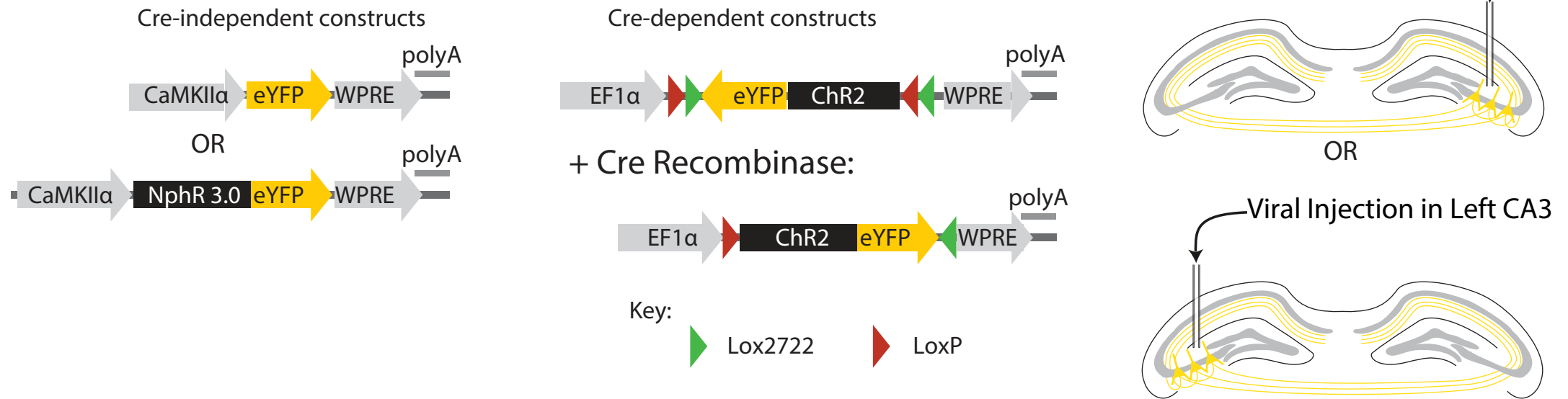
controls *P<0.05, ** P<0.01, *** P<0.001. Error bars represent s.e.m. Panel B-D adapted from

(**6**).

L   R
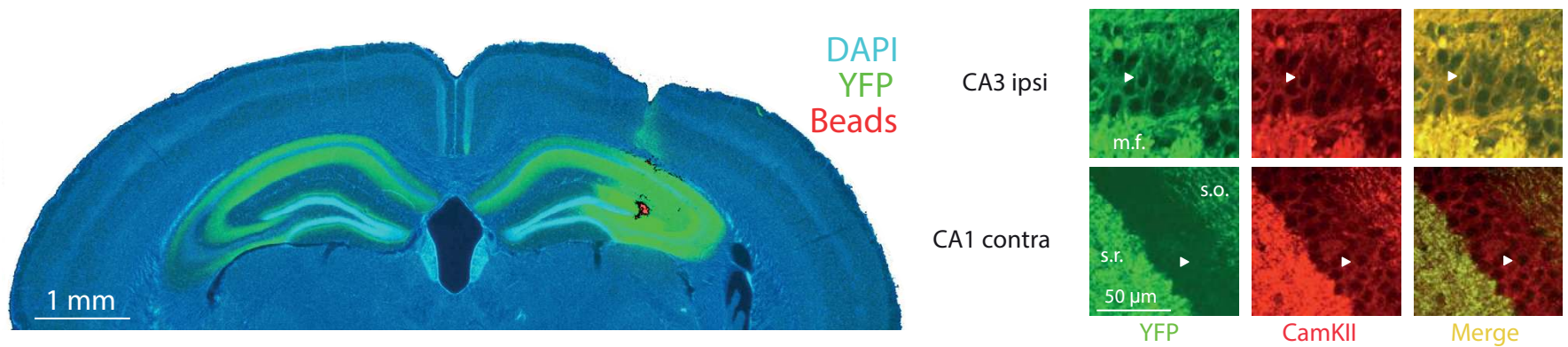
CA1

DG

VHC

CA3

• DG granule cell

▼ CA3 pyramidal cell

Y CA1 pyramidal cell

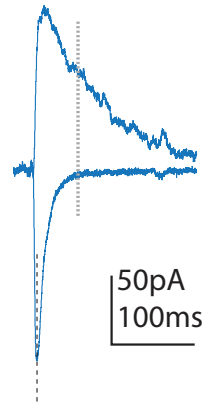CA1　　　　　　　　CA1

VHC

Left CA3　　　　Right CA3

NMDAR
subunits

GluN1

GluN2A

GluN2B

GluN2B
c-tail

AMPAR
subunits

GluA1

GluA2

GluA3

CaMKII

CA1

A

Cre-independent constructs

CaMKIIα — eYFP — WPRE — polyA

OR

CaMKIIα — NphR 3.0 — eYFP — WPRE — polyA

Cre-dependent constructs

EF1α — eYFP · ChR2 — WPRE — polyA

+ Cre Recombinase:

EF1α — ChR2 — eYFP — WPRE — polyA

Key:
▶ Lox2722   ▶ LoxP

Viral Injection in Right CA3

OR

Viral Injection in Left CA3

B

DAPI
YFP
Beads

1 mm

CA3 ipsi

m.f.

CA1 contra

s.o.
s.r.

50 μm

YFP   CamKII   Merge

A

CA1

L   R   CA3

optical
illumination   CA1   recording
                        s.p.
                        s.r.
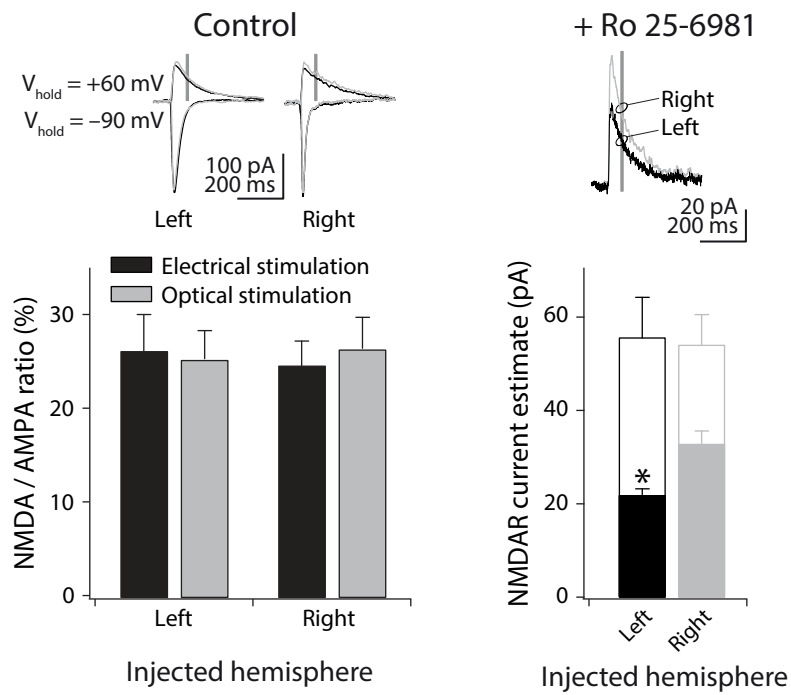from CA3
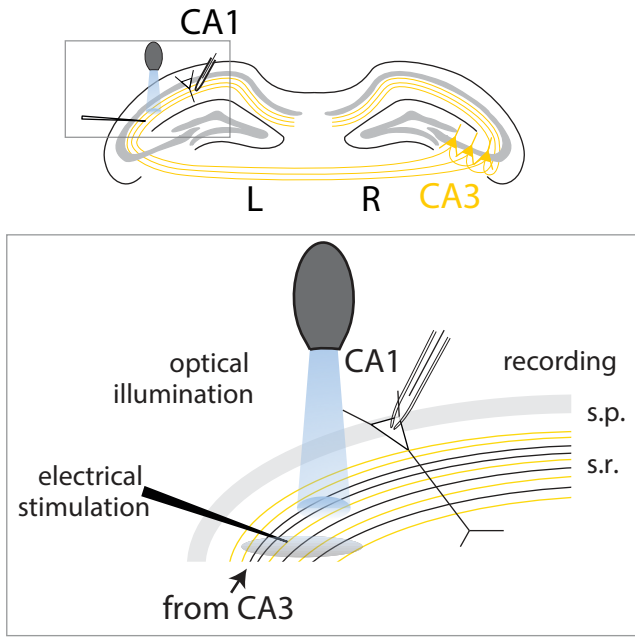
— projections expressing ChR2-eYFP
— projections not expressing ChR2-eYFP

B

200 pA
500 ms

C

50pA
100ms

D

Control   + Ro 25-6981

$V_{hold} = +60$ mV
$V_{hold} = -90$ mV

100 pA
200 ms

Left   Right

Right
Left

20 pA
200 ms

■ Electrical stimulation
□ Optical stimulation

NMDA / AMPA ratio (%)

Left   Right

Injected hemisphere

NMDAR current estimate (pA)

*

Left   Right

Injected hemisphere

A

CA1

L   R   CA3

optical illumination

CA1   recording

s.p.

s.r.

electrical stimulation

from CA3

— projections expressing ChR2-eYFP
— projections not expressing ChR2-eYFP

B

5 mV

50 ms

50 mV

200 pA

C

Rec.   CA1

CA3   L   R

Normalized EPSP slope (%)

Pairing

2 mV
20 ms

200

150

100

50

0

0   10   20   30   40   50

Time (min)

▲ Electrical stimulation
● Optical stimulation

Left CA3
injected

CA1   Rec.

L   R   CA3

Normalized EPSP slope (%)

Pairing

2 mV
20 ms

200

150

100

50

0

0   10   20   30   40   50

Time (min)

▲ Electrical stimulation
● Optical stimulation

Right CA3
injected

A

CA1

L   R   CA3

optical illumination   CA1   recording

s.p.

electrical stimulation

s.r.

from CA3

— projections expressing ChR2-eYFP
— projections not expressing ChR2-eYFP

B

Induction: 100 stimuli at 100 Hz

500 µV
10 ms

C

Left CA3 injected

1
2
1
2
1 mV
10 ms

Right CA3 injected

1
2
1
2
1 mV
10 ms

Normalised fEPSP slope (%)

200

150

100

50

0

2

1

▲ control - electric stim.
● left input - light stim.

0 10 20 30 40 50
Time (min)

200

150

100

50

0

2

1

▲ control - electric stim.
● right input - light stim.

0 10 20 30 40 50
Time (min)

200

150

100

50

0

**

control left-input control right-input

Figure 6

Figure 7